*Environ. Sci. Technol.* **2008,** *42,* 7655–7662

# Apportionment of Primary and Secondary Organic Aerosols in Southern California during the 2005 Study of Organic Aerosols in Riverside (SOAR-1)

KENNETH S. DOCHERTY,[†,‡] ELIZABETH A. STONE,[∥] INGRID M. ULBRICH,[†,‡] PETER F. DeCARLO,[†,§,○] DAVID C. SNYDER,[∥] JAMES J. SCHAUER,[∥] RICHARD E. PELTIER,[⊥,◆] RODNEY J. WEBER,[⊥] SHANE M. MURPHY,[#] JOHN H. SEINFELD,[#] BRETT D. GROVER,[▽,¶] DELBERT J. EATOUGH,[▽] AND JOSE L. JIMENEZ*[,†,‡]

*Cooperative Institute for Research in Environmental Sciences and Department of Chemistry and Biochemistry, Department of Atmospheric and Oceanic Sciences, University of Colorado, Boulder, Colorado, Environmental Chemistry and Technology Program, University of Wisconsin, Madison, Wisconsin, School of Earth and Atmospheric Sciences, Georgia Institute of Technology, Atlanta, Georgia, Division of Chemistry and Chemical Engineering, California Institute of Technology, Pasadena, California, and Department of Chemistry and Biochemistry, Brigham Young University, Provo, Utah*

*Received March 21, 2008. Revised manuscript received July 30, 2008. Accepted July 31, 2008.*

Ambient sampling was conducted in Riverside, California during the 2005 Study of Organic Aerosols in Riverside to characterize the composition and sources of organic aerosol using a variety of state-of-the-art instrumentation and source apportionment techniques. The secondary organic aerosol (SOA) mass is estimated by elemental carbon and carbon monoxide tracer methods, water soluble organic carbon content, chemical mass balance of organic molecular markers, and positive matrix factorization of high-resolution aerosol mass spectrometer data. Estimates obtained from each of these methods indicate that the organic fraction in ambient aerosol is overwhelmingly secondary in nature during a period of several weeks with moderate ozone concentrations and that SOA is the single largest component of $PM_1$ aerosol in Riverside. Average SOA/OA contributions of 70−90% were observed during midday periods, whereas minimum SOA contributions of ∼45% were observed during peak morning traffic periods. These results are contrary to previous estimates of SOA throughout the Los Angeles Basin which reported that, other than during severe photochemical smog episodes, SOA was lower than primary OA. Possible reasons for these differences are discussed.

## Introduction

Aerosols are of interest due to their roles in several atmospheric processes including radiative forcing, heterogeneous reactions, and regional visibility degradation, as well as their negative impact on human health. The impact of particles on these and other atmospheric processes are dependent on particle size, the majority being strongly correlated with fine particles ($PM_{2.5}$ or $PM_1$), and many also depend on chemical composition. In particular, the organic fraction ("organic aerosols", OA), which typically constitutes a significant fraction of fine particle mass (*1*), is a poorly characterized aggregate of thousands of individual compounds either emitted directly in the particle-phase ("primary" OA, POA) or formed in the atmosphere from gas-to-particle conversion ("secondary" OA, SOA). Most of these compounds are not amenable to detection by currently available speciation techniques, which can identify only a small fraction of aerosol organics at the molecular level (*2*). The lack of molecular characterization of a large fraction of the mass is particularly important for SOA.

During the Study of Organic Aerosols in Riverside (SOAR-1), a variety of state-of-the-art instrumentation was assembled at the Air Pollution Research Center on the campus of the University of California-Riverside from July 18 through August 14, 2005 to investigate the chemical composition of ambient OA, representing, to our knowledge, the most complete set of OA field instruments at one location to date. Riverside is located ∼80 km inland of the urban center of Los Angeles (LA). Due to its proximity to LA and the meteorology, topography, and intense emissions characteristic of the LA basin, Riverside and the surrounding areas are characterized by poor air quality, consistently rating as the worst in the United States for 24 h average fine particle concentrations both on short-term and annual bases (*3*).

Here, we estimate the fraction of SOA in fine particles using five methods including the elemental carbon (EC) and carbon monoxide (CO) tracer methods, water soluble organic carbon (WSOC) content, chemical mass balance (CMB) source apportionment of organic molecular markers (MMs), and positive matrix factorization (PMF) of high-resolution time-of-flight aerosol mass spectrometer (HR-ToF-AMS) organic mass spectra. Results obtained from each of these methods indicate that SOA contributes the majority of organic mass during a period that cannot be described as a "photochemical episode". Estimates obtained from each of these methods are higher than previous SOA estimates in locations throughout the LA Basin including Riverside and surrounding areas.

## Experimental Section

**General.** All measurements were conducted in Riverside, California at the Air Pollution Research Center on the campus of the University of California-Riverside (33°58′18.40″N, 117°19′21.41″W). During SOAR-1 (July 18 through August 14, 2005), the Riverside area was characterized by moderate

* Corresponding author e-mail: jose.jimenez@colorado.edu.
† Cooperative Institute for Research in Environmental Sciences.
‡ Department of Chemistry and Biochemistry, University of Colorado.
§ Department of Atmospheric and Oceanic Sciences, University of Colorado.
∥ University of Wisconsin.
⊥ Georgia Institute of Technology.
# California Institute of Technology.
▽ Brigham Young University.
○ Currently at Paul Scherrer Institut, Switzerland.
◆ Currently at NYU School of Medicine, Department of Environmental Medicine, Tuxedo, New York.
¶ Currently at United States Environmental Protection Agency, National Exposure and Research Laboratory, Durham, North Carolina.

10.1021/es8008166 CCC: $40.75 
Published on Web 09/23/2008

ozone concentrations (average peak daily ozone concentration in Riverside = 86 ppb; range 48−141 ppb). All times refer to Pacific Standard Time.

**Sunset Semicontinuous EC/OC Measurements.** $PM_{2.5}$ organic carbon (OC) and elemental carbon (EC) concentrations were measured hourly using both standard (*4*) and dual-oven (*5*) Sunset semicontinuous carbon monitors (Sunset Laboratories, Tigard, OR).

**Filter-Based Measurements.** Filter samples were collected for source apportionment by CMB of solvent-extractable organic MMs (*2*). Details regarding particle collection, filter extraction, chemical analysis, and CMB procedures are similar to those presented in Stone et al. (*6*) with a few exceptions noted below.

Filter samples for CMB were collected daily according to the following schedule: 0400−0900; 0900−1400; 1400−1900; 1900−0400. Weekday samples collected on 7/26−7/28 and 8/2−8/4 and weekend samples collected on 7/30 and 8/6−8/7 were composited based on this schedule. For this analysis, weekday and weekend CMB source apportionment results were further composited to yield results irrespective of day of week. These samplers were not denuded. As a result, filter OC concentrations are likely inflated through adsorption of semivolatile gas-phase species. To obtain a conservative estimate of "other" OC, the results of CMB source apportionment were used in conjunction with coinciding standard Sunset OC concentrations (i.e., "other" OC = $OC_{Sunset}$ − primary OC (POC)). If we were to instead use the CMB filter OC concentrations for this estimate, other OC increases by ∼7% likely as a result of these adsorption artifacts.

**Particle-Into-Liquid-Sampler (PILS) Organic Measurements.** Water soluble OC (WSOC) and total OC were measured by a PILS-WSOC and PILS-OC, respectively (*7*). WSOC was measured continuously every 6 minutes from 7/18−7/27 and 7/30−8/15. The PILS-OC measured total OC continuously from 7/27−7/30 at the same rate. Further details are provided elsewhere (*7*).

**HR-ToF-AMS Measurements.** Nonrefractory $PM_1$ aerosols were measured by an Aerodyne HR-ToF-AMS from 7/14−8/10. Details regarding the HR-ToF-AMS are provided elsewhere (*8*).

**Data Analysis.** Conversion of carbon mass concentrations. Measured concentrations of OC, WSOC, and water insoluble organic carbon (WIOC) were converted to organic mass (OM) concentrations prior to calculating SOA fractions. POC and WIOC were converted using a factor of 1.2 $\mu$gOM/$\mu$gOC, whereas secondary OC (SOC) and WSOC were converted to secondary organic mass (SOM) using a factor of 1.8 $\mu$gOM/$\mu$gOC (*9*). In Supporting Information (SI) Table S-2, we explore the sensitivity of calculated SOA/OA ratios to the applied SOM/SOC conversion factor using additional conversion factors of 1.6 and 2.0 $\mu$gOM/$\mu$gOC. As this table shows, SOA/OA ratios vary only a few percent when these alternate conversion factors are used.

**HR-ToF-AMS.** Unit-resolution (UMR) ToF-AMS data were analyzed using established procedures for analysis of AMS data via customized data analysis software (Squirrel) (*10*). An AMS collection efficiency (CE) of 0.5 was used for all species, typical of aerosols measured in urban locations with similar composition (*11, 12*) and verified with intercomparisons with other collocated instruments. The AMS response may be slightly biased toward POA (*13, 14*), and these SOA/OA estimates should be considered lower limits. High-resolution (HR) ToF-AMS data were analyzed using a custom data analysis module (Pika) developed in our group (*8*) in Igor (Wavemetrics, Lake Oswego, OR).

**PMF Analysis.** AMS organic mass spectra were analyzed by PMF to identify the major components of $PM_1$ OA. PMF is a variant of factor analysis with nonnegative constraints on factor elements and has been described in detail elsewhere (*15*). Its application to AMS spectra has been investigated in detail recently (*16, 17*). HR ($m/z \leq 100$ and UMR ($m/z > 100$) organic mass spectra were combined for PMF analysis. PMF2 (v4.2) was run in robust mode via a custom panel in Igor (*16*).

**Lack of Important Biomass Burning (BB) Impact.** Although the LA area is at times impacted by smoke from large wildfires that can increase $PM_{10}$ levels in the basin by 300−400% (*18*), fires throughout Southern California during SOAR-1 were small in size, short in duration, and not in the vicinity of the sampling location, according to the MODIS Active Fire Detections database (http://maps.geog.umd.edu/firms/maps.asp). This is supported by measurements by a collocated aerosol time-of-flight mass spectrometer that did not observe significant PM contributions from biomass burning/biofuel combustion sources (*19*). Moreover, $m/z$ 60 (a BB tracer) in the AMS during the study (see SI Figure S1) as well as measured concentrations of the MM levoglucosan were low during SOAR-1 (see below).

## Results and Discussion

**EC-Tracer Method.** This method assumes that EC results predominantly from combustion processes and can be used as a tracer for primary aerosol (*20*). POC is estimated by its proportionality with EC as

$$\mathrm{POC} = [(\mathrm{OC/EC})_p \times \mathrm{EC}] + \mathrm{NCPOC}, \quad (1)$$

where NCPOC is noncombustion POC, and SOC is determined by difference:

$$\mathrm{SOC} = \mathrm{OC} - \mathrm{POC}. \quad (2)$$

The simple appearance of this method is belied by significant complexities associated with determining the coefficients $(OC/EC)_p$ and NCPOC in eq 1, which are traditionally obtained by linear regression analysis of EC and OC data during periods that are deemed "not impacted by SOC." NCPOC contributions (that are not correlated with EC due to similar source locations and/or activity patterns) are small relative to errors associated with the EC-tracer method (*21*). Therefore, they are lumped with SOC in the following EC-tracer calculations.

For ambient sampling, the correct $(OC/EC)_p$ should be $\Sigma(OC)/\Sigma(EC)$ for all primary sources. Therefore, OC and EC data used in the regression analysis must be carefully selected to limit contributions from SOC, which would incorrectly inflate both $(OC/EC)_p$ and POC. For areas like the LA Basin this is not trivial. Strader et al. (*22*) estimated $(OC/EC)_p$ using regression analysis of data collected in California's San Joaquin Valley and found that isolating a single period that was not impacted by photochemistry was "a dangerous proposition" due the long residence times of $PM_{2.5}$. Zhang et al. (*23*) showed that in Pittsburgh this method of estimating $(OC/EC)_p$ led to a large overestimation of POA since SOA was always a significant fraction of the OA. This technique typically neglects variations in $(OC/EC)_p$ throughout the day that can appear due to, e.g., variations in diesel and gasoline vehicle fractions, which may lead to some errors in the estimated diurnal profiles (*24*), as discussed below.

To explore the range of SOA contributions during SOAR-1, EC-tracer calculations were conducted using a range of $(OC/EC)_p$ values estimated both using available emissions inventory data and from the literature. $(OC/EC)_p$ ratios used to obtain SOA/OA estimates by the EC-tracer method, in addition to details regarding their determination, are presented in SI Table S1. $(OC/EC)_p$ estimates were calculated using available vehicle emissions inventories for the South Coast Air Basin and emission factors determined in several recent tunnel studies in California. Due to the high concentration of primary emissions observed in tunnel studies which favor partitioning of semivolatile OC to the particle

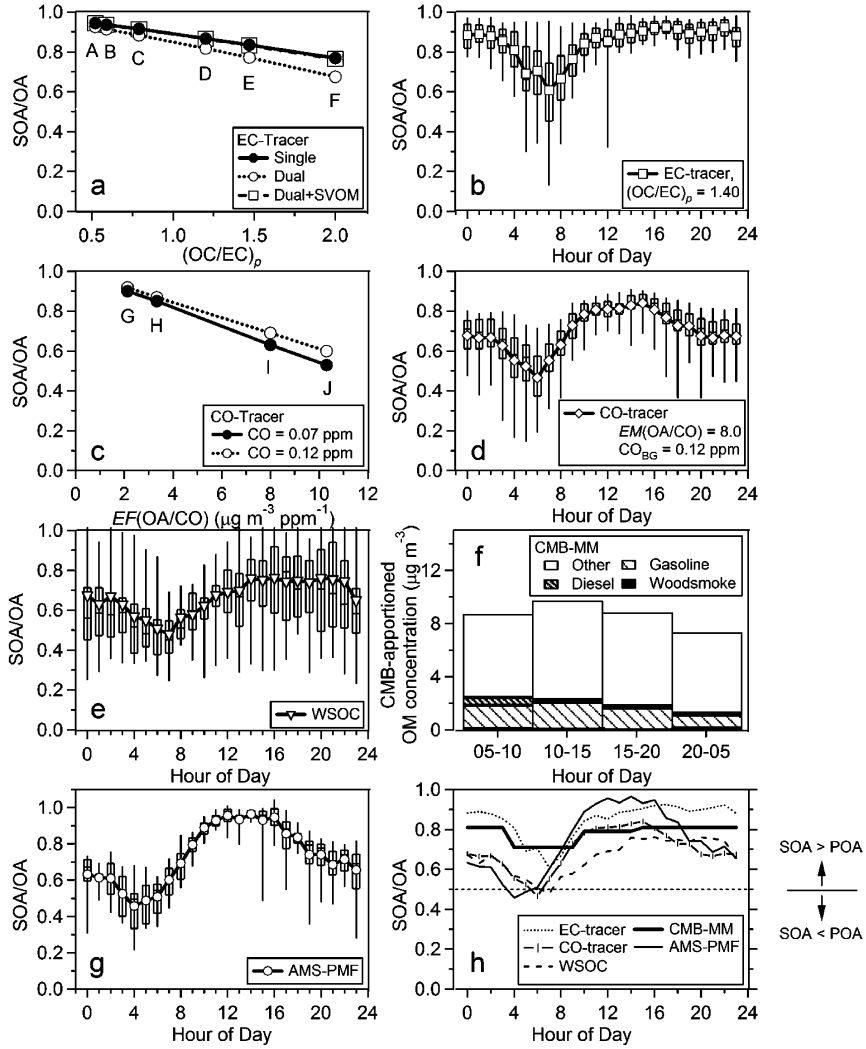


**FIGURE 1. Estimated SOA/OA ratios and results of CMB OA apportionment during SOAR-1. Figure 1a shows campaign-average SOA fractions from the EC-tracer method as a function of $(OC/EC)_p$. Applied $(OC/EC)_p$ values for (A−C) were calculated using emissions ratios measured in several Caldecott Tunnel studies (*26*−*28*). Literature values for $(OC/EC)_p$ were obtained from (D) AMS spectral deconvolution (*23*), (E) radiocarbon determinations (*30*), and (F) traditional regression analysis of semicontinuous OC and EC data (*29*). Figure 1b shows the diurnal profile of SOA/OA ratios obtained from the EC-tracer method. Figures 1c and 1d show average SOA/OA ratios obtained from the CO-tracer method as a function of EF(OA/CO) and the diurnal profile of SOA/OA ratios calculated using our central estimate (EF(OA/CO)=8.0 and $CO_{BG}$ = 0.12 ppm), respectively. Figure 1e shows the diurnal profile of SOA/OA ratios obtained from the WSOC method. Figure 1f presents results of CMB OA apportionment while Figure 1g shows the diurnal profile of SOA/OA ratios obtained from PMF. Finally, Figure 1h compares SOA/OA estimates from all methods in the same plot to facilitate comparison.**

phase, resulting emission factors should be considered as an upper bound to OC/EC for tunnel studies. $(OC/EC)_p$ was calculated from emissions data as follows:

$$(OC/EC)_p = [(OC_{diesel}+OC_{gasoline})/(EC_{diesel}+EC_{gasoline})] = [(EF_{OC,diesel}{}^{*}\,DFU_{diesel}) + (EF_{OC,gas}{}^{*}\,DFU_{gas})]/[(EF_{EC,diesel}{}^{*}\,DFU_{diesel}) + (EF_{EC,gas}{}^{*}\,DFU_{gas})] \quad (3)$$

where $DFU_{diesel}$ and $DFU_{gas}$ are average daily fuel use (kg $day^{-1}$) for diesel and gasoline, respectively, within the South Coast Air Basin for 2005 (*25*) and $EF_x$ (g OC $kg^{-1}$ fuel) are emission factors calculated from recent tunnel studies in California (*26*−*28*).

Estimates from the ambient linear regression method are likely to constitute an upper bound for $(OC/EC)_p$ due to the difficulty involved with eliminating SOC contributions (*22*). Recent studies in both Pittsburgh (*29*) and the Los Angeles basin (*21*) report $(OC/EC)_p \sim 2$. Somewhat lower $(OC/EC)_p$ estimates have been obtained by other methods including $^{14}C/^{12}C$ analysis of EC and OC samples (*30*) and by comparing the fraction of oxygenated OA resulting from AMS mass spectral deconvolution with average SOA fractions calculated by the EC-tracer method (*23*). Due to the use of $^{14}C/^{12}C$ ratios in Szidat et al. (*30*), this estimate should have lower potential inflationary errors of incorporating SOC, although it applies to a European vehicle fleet which has some differences with that of California. In Zhang et al. (*23*), equivalent SOA fractions were obtained from both methods using an $(OC/EC)_p = 1.20$, which is equivalent to applying the regression method after subtracting the AMS-estimated SOA from the ambient OA during high POA periods. These latter literature estimates may be still higher than the tunnel studies due to the incorporation of POA from sources other than vehicle emissions, or some fast SOA formation from anthropogenic precursors (*31*).

Using each literature and emissions-based $(OC/EC)_p$ estimate, average POC and SOC concentrations were calculated using campaign-long average OC and EC concentrations measured by both Sunset instruments. Corresponding SOA estimates are shown in Figure 1a as a function of $(OC/EC)_p$. Two sets of results are shown for the dual-oven Sunset

instrument showing the impact of measured semivolatile organic mass (SVOM) concentrations (*5*). As Figure 1a shows, SOA contributes a majority of $PM_{2.5}$ organic mass when averaged over the entire length of the sampling period. Conservative estimates of SOA fraction using $(OC/EC)_p = 2.0$ result in a SOA/POA ratio of ≥2:1, whereas use of a more reasonable $(OC/EC)_p \sim 1.4$ gives corresponding ratios of ≥4:1. Using $(OC/EC)_p$ ratios from tunnel studies results in a SOA/POA ratio ≥4.5:1. The diurnal plot of SOA/OA ratios calculated from the EC-tracer method using EC/OC data from the standard Sunset instrument and an $(OC/EC)_p = 1.4$ is shown in Figure 1b. This calculation provides an overall average SOA/OA ratio 84 ± 18%, with a minimum during the morning rush hour as expected.

**CO-Tracer Method.** The CO-tracer method is analogous to the EC-tracer method and has been used recently to estimate the fraction of SOA in $PM_1$ using collocated measurements of AMS organics and CO (*32*). Similar to the EC-tracer method, the CO-tracer method apportions POA mass using a tracer of primary emissions along with an estimated emissions ratio. However, due to different OA/CO and OA/EC emission ratios of different sources such as diesel and gasoline vehicles (*24*), the results of the CO-tracer method have some differences with those from the EC-tracer method. These differences are an indication of the uncertainty in the estimates for this type of simplified method. POA concentrations are calculated using

$$\mathrm{POA} = (\mathrm{OA/CO})_p \times \Delta\mathrm{CO} + \mathrm{NCPOC} \quad (4)$$

where ΔCO is the CO enhancement above background (i.e., $CO_i - CO_{BG}$) and $(OA/CO)_p$ is the POA to CO emissions ratio. SOA concentrations are estimated as the difference between the measured OA and the summed POA similar to eq 2 above.

$(OA/CO)_p$, like $(OC/EC)_p$, needs to be estimated with similar methods, e.g., from regression analysis of "less processed" air (i.e., air masses where OA concentrations are thought to be dominated by primary combustion sources). This ratio has previously been estimated in a variety of locations including Pittsburgh (*23*), New England (*33*), and Tokyo (*32*) with values ranging from 4.3−14.4 $\mu g\ m^{-3}$ OA $ppm^{-1}$ CO. The minimum within this range was determined by Zhang et al. (*23*) based on regression of ambient CO and hydrocarbon-like aerosol obtained from deconvolution of AMS mass spectra and is higher than OA/CO emission ratios of 2.13 (*26*) and 3.33 $\mu g\ m^{-3}\ ppm^{-1}$ (*28*) obtained from California tunnel studies. The regression of total OA during high POA periods yields an $(OA/CO)_p = 10.3\ \mu g\ m^{-3}\ ppm^{-1}$ during SOAR-1. As with the EC-tracer method, estimates based on total ambient OA are very likely biased high due to the presence of some SOA that also shows strong correlation with anthropogenic tracers (*33*) and should be considered upper limits. We use a ratio of $8.0\ \mu g\ m^{-3}\ ppm^{-1}$ and $CO_{BG} = 0.12$ ppm (*34*) for our central estimate, and explore the sensitivity to the more conservative estimate obtained using a ratio of 10.3 and $CO_{BG} = 0.07$ ppm. We neglect changes in $(OA/CO)_p$ with time-of-day that can introduce some error in the diurnal profiles (*24*). CO produced through oxidation of volatile organic compounds is estimated to make a minimal contribution (∼1%) to excess CO in the South Coast Air Basin (*35*).

Figure 1c shows SOA/OA ratios resulting from the CO-tracer method as a function of $(OA/CO)_p$ at background CO concentrations of 0.07 and 0.12 ppm. As this plots shows, the CO-tracer method again indicates that OA measured during SOAR-1 is dominated by SOA. The average SOA/OA ratio obtained from the central estimate is 69% ± 24%. This estimate decreases by ∼16% when CO-tracer method calculations were repeated using the more conservative assumptions. Similarly, using the average ratio from tunnel studies and $CO_{BG} = 0.12$ increases the SOA/OA ∼20% compared to the central estimate. The diurnal profile of SOA/OA ratios calculated using our central estimate of the CO-tracer method is presented in Figure 1d. Maximum SOA/OA ratios >80% are observed during mid-day hours (1100−1600) and later steadily decline to a midnight value of ∼67%. As expected, minimum contributions from SOA were observed during the morning rush hour with an absolute minimum of ∼47% at 0600.

**SOA Estimate from WSOC Content.** In polluted regions, compounds comprising WSOC are either mainly emitted from BB sources or formed via secondary atmospheric processes (*36*). SOA species are polar and typically highly oxygenated, leading to much higher water solubility than for reduced anthropogenic POA species. Due to the small fraction of BB OA during SOAR-1, most of the WSOC should be due to SOA species. In order to accurately use WSOC as a surrogate for SOC, measured WSOC concentrations must be adjusted to account for the water-insoluble fraction of oxygenated organic carbon (OOC). A conservative estimate of this fraction is obtained here from Kondo et al. (*37*) where it was estimated that 6−26% of summer OOC in Tokyo was water-insoluble based on direct comparisons between PILS-WSOC and Quadrupole AMS measurements. However, water- insoluble SOA fractions as large as 60% have recently been reported (*38*) which if applicable in CA would result in a low bias in our SOA estimates by this technique.

A WSOC/OC ratio of 0.56 ± 0.05 was obtained from PILS-WSOC and PILS-OC measurements during SOAR-1 (*7*). We estimate the SOA fraction using this ratio corrected for water-insoluble OOA content and converted to OM using factors discussed above. A conservative 24 h average SOA/OA estimate of 66 ± 8% is obtained using the 6% water-insoluble OOC correction, which increases by ∼9% when the 26% water-insoluble OOC correction is instead applied. The diurnal profile of SOA/OA estimates from the WSOC method using the 6% water-insoluble OOC correction is shown in Figure 1e. A global minimum of 48% is obtained at 0700 with maximum values of ∼75% occurring at mid-day. A final concern is the potential contribution of highly water soluble organics from BB to WSOC concentrations, which would artificially increase this SOA estimate. As discussed previously, the impact of BB throughout the LA basin during SOAR-1 was small. Using the results of CMB analysis (below) we estimate that the contribution of BB to WSOC and total OA is ≤1% using a WSOC/OC emissions ratio of 0.71 (*39*). As a result, the estimate for SOA fraction obtained from this method would change little if the BB contribution were to be subtracted.

**CMB of Organic Molecular Markers.** CMB models are based on the mass conservation of individual organic species. The mass conservation equations are written as the matrix product of unknown time series of source contributions and known source profiles equaling the time series of known concentrations of a set of molecular marker species observed in ambient aerosol and are solved with the effective variance least-squares method. CMB models have been used to apportion source contributions to ambient $PM_{2.5}$ in numerous locations including the LA Basin (e.g., refs *2, 6*).

Here CMB is applied to selected OA tracer species that are solvent extractable and elutable from a gas chromatography (GC) column, which applies to only a limited amount of particle-associated organic compounds (*2*). However, this small subset is sufficient to act as tracers of major primary sources (*2*), including fossil fuel, coal, natural gas, and biomass combustion, vegetative detritus, and meat smoke. Hopanes and *n*-alkanes were included in the CMB model as markers for fossil fuel combustion (*40*). Markers for woodsmoke including levoglucosan (*41*) were also measured and included in the CMB model. Markers for coal, natural gas combustion, meat smoke, and vegetative detritus were either

not observed or negligible and were not included. The measured concentrations of selected $PM_{2.5}$ organic marker species included in the CMB model are shown in SI Figure S2 by filter composite period. On average, the concentrations of all quantified organic species and CMB tracer species compose <5 and <0.5% of total OA, respectively.

Molecular markers for SOA, comprised of organic compounds formed in the atmosphere through condensation or gas-to-particle conversion, are difficult to quantify with GC analysis and are not typically apportioned by CMB models. An upper bound estimate of SOA, however, can be obtained by difference:

$$SOA_{CMB} = OA - \sum (POA_i) \quad (5)$$

where $\Sigma(POA_i)$ is the sum of the POA apportioned to all sources (*2*).

Results of CMB OA apportionment are shown in Figure 1f. For each composite period, CMB apportioned >95% of POC to fossil fuel emissions, with the majority (~64%) being attributed to emissions from gasoline vehicles. The small remainder (<5%) of the POC in each composite period was apportioned to BB (~0.1 $\mu g\,m^{-3}$ daily average). In each period, the total CMB-apportioned POA makes up a relatively small fraction of measured $PM_{2.5}$ OA. In contrast, the "other" organics consistently contributes the largest amount of mass (77%; range 72−83%). Recent studies have indicated that the bulk of this fraction is SOA, which is also consistent with the estimates of the four other methods presented here. For example, CMB source apportionment of $PM_{2.5}$ OA in six southeastern United States locations observed highest contributions of "other" organic in all locations during July, coinciding with peak photochemical activity (*42*). Additionally, strong correlations have been observed between this fraction and the sum of secondary inorganics (*42*) and ambient WSOC concentrations (*6*).

**PMF Analysis of HR-ToF-AMS Data.** In contrast to most of the methods discussed above that apportion SOA as the difference between measured OA and apportioned POA, PMF explicitly identifies individual OA components. PMF and similar advanced factor analysis models have previously used Quadrupole AMS data to determine OA sources in urban regions of Pittsburgh and Zurich, Switzerland (*16, 17*). The use of HR data results in greater differentiation between the spectra of the OA components, which has been shown to enhance AMS OA component separation using PMF (*16*).

The number of factors identified in the PMF solution was selected by examining both mathematical PMF diagnostics and interpretability of the identified factors based on similarity with AMS source spectra and time series of independent tracers (*16, 17, 43*). Reduced (hydrocarbon-like, HOA) components were classified as primary, OOA components were classified as secondary, and one small (~5% contribution to $PM_1$ OA mass) component was classified as "other" based on these comparisons (*16, 17, 23, 44*). Finally, the mass concentration of SOA was calculated as the sum of individual secondary factor mass concentrations. Some fresh SOA can have a reduced spectrum and may be incorrectly classified as POA by this method (*45*).

Over the entire sample period, the average SOA/OA ratio obtained from PMF analysis is 74 ± 19%. The diurnal profile of SOA/OA ratios from PMF-AMS analysis is shown in Figure 1g. Minimum SOA/OA ratios ~45% are again observed during the morning rush hour period. Overall, this profile is very similar to that obtained with the CO-tracer method. However the EC-tracer method apportions SOA slightly differently throughout the evening/night, with higher SOA/OA ratios during those periods. This may result from higher $(OC/EC)_p$ during the night due to reduced diesel traffic at that time (*24*).

In order to facilitate comparison, Figure 1h shows the diurnal profiles of SOA/OA estimated by all methods. Diurnal cycles of these ratios are similar with maximum SOA/OA ratios of 70−90% estimated by each method during the early afternoon. Minimum SOA/OA ratios obtained from each method do not fall below 45% during any 1 h period. The differences in the diurnal profiles are indicative of current uncertainties in the estimation of SOA from field measurements.

Dominant contributions of SOA to OA also do not appear to be limited to distant locations at the eastern part of the LA basin. AMS mass spectra from Riverside and Pasadena (14 km NNE of downtown LA) exhibit a high degree of similarity and suggest that Pasadena OA is also characterized by high SOA/OA ratios. SI Figure S3 compares Riverside UMR OA mass spectra averaged from 7/28 to 8/3 with that measured by a C-ToF-AMS at the California Institute of Technology (Caltech) in Pasadena over the same time period. The degree of OA oxidation, estimated using the ratio of $m/z$ 44 (oxidized OA marker fragment) to total organics (*46*) is similar (even slightly higher in Pasadena), indicating a high degree of oxidation in OA observed in both locations, likely explained by rapid SOA formation (*31*). In support of this observation, we note that although estimates by Pandis et al. (*47*) are significantly lower than those obtained during SOAR-1, similar SOA contributions to total organics were calculated for Rubidoux and Burbank, which are located near Riverside and Pasadena, respectively. Back-trajectories shown in SI Figure S4 indicate that air masses arriving at each location at 1:00 p.m. were transported from the west through the Los Angeles urban area and spent several hours to a day over the urban area before their arrival at either measurement site.

**Comparison with Previous Estimates of SOA in this Area.** Numerous studies have previously estimated the SOA in the LA Basin using a variety of methods including modeling (*47−51*), CMB-MM (*2, 52*), and the EC-tracer method (*20, 21, 53*). Figure 2 presents several previous estimates of SOA/OA in this region along with the five estimates from this study.

There is considerable variation in SOA estimates reported by previous studies much of which is likely due to differences in sampling season, location, and duration. Common to all these previous studies, however, is that POA contributes the majority of OA over extended periods. Unlike the current study, SOA/OA ratios >50% have previously been reported to occur only during severe photochemical smog events (SPSE), characterized by ozone concentrations in excess of ≥200 ppb. Schauer et al. (*52*) reported results of CMB source apportionment on filter samples collected throughout the LA basin during a two-day photochemical smog event in 1993. The eastern-most sampling location was Claremont, California, ~50 km inland of LA where CMB apportioned ~75% of measured OA as SOA. Similarly, Turpin et al. (*20*) observed several photochemical smog events in Claremont. During the events observed by Turpin et al., SOA/OA ratios were estimated to be greater than 50% for a few hours following the daily maximum ozone concentration. Both of these studies reported the predominance of SOA over short time periods with high photochemistry, which span between a few hours and two days. If we exclude these limited photochemical events, however, previous summer studies taken together indicate an average SOA fraction below 50% (*20, 21, 47, 53*). However, SOA fractions estimated during the multiweek SOAR-1 study are substantially higher (74% based on the average of the five methods) than estimated by these previous studies despite the fact that ozone concentrations in this part of the basin were not significantly elevated during SOAR-1.

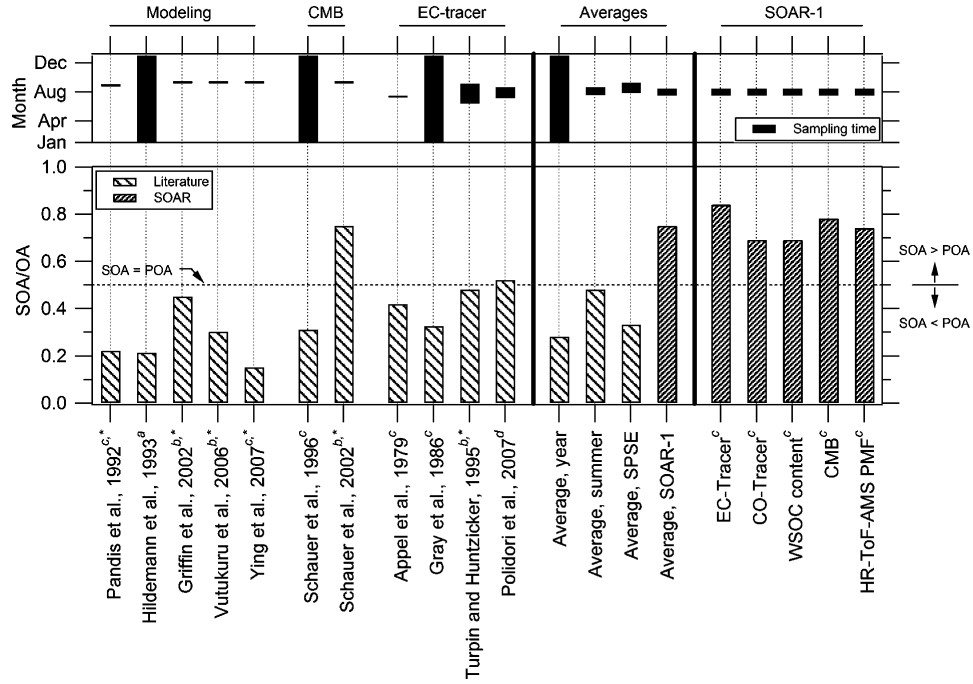


**FIGURE 2. Comparison of SOA/OA ratios determined during SOAR-1 with previous measurements throughout the Eastern LA Basin using a range of analytical methods. The bottom shows the reported SOA fraction, whereas the top shows the time and duration of sampling corresponding to each estimate. Subscript letters indicate sampling location *a*) multiple locations; *b*) Claremont/Azusa; *c*) Riverside/Rubidoux; and *d*) undisclosed location (due to confidentiality) ~50 km east of LA, and * indicates an estimate obtained during a photochemical smog event.**

Different SOA estimates between SOAR-1 and previous studies may have a number of underlying explanations including (1) atypical atmospheric conditions during the SOAR-1 campaign; (2) problems in methods used to obtain previous SOA estimates; and (3) genuine changes in organic aerosol sources. Differences are not likely due to anomalous conditions during SOAR-1. SI Figure S5 presents daily average $PM_{2.5}$, ozone, CO, and $NO_x$ concentrations measured in Rubidoux (~10 km west of Riverside) along with total acres burned in fire events in Riverside and San Bernardino Counties for the period 7/15 to 8/15/2000−2006, whereas Figures S6 and S7 in the SI compare the meteorological conditions for these same periods. For 2005, ozone is very similar to previous years suggesting a likely similar contribution of SOA (*54*). While CO is lower, $NO_x$ is very similar to previous years, indicating that the POA contribution was not drastically smaller than in 2000−2004. Since the main source of CO is gasoline vehicles, if we increase their CMB-estimated POA contribution proportional to the difference in CO, we would obtain a CO-corrected SOA estimate of 68% according to CMB, which should be treated as a lower limit since gasoline vehicles are also an important source of $NO_x$, and since the additional gasoline emissions would also increase SOA.

Some of this difference however can be explained by problems in the methods applied to obtain the previous estimates. For instance, large uncertainties in the Pandis et al. (*47*) SOA estimates were attributed to understated basin-wide emissions of gas-phase organics and discrepancies in experimentally determined SOA yields. Doubling the VOC emissions increased SOA fractions in Claremont by a factor of 2.3 and improved the correlation between projected and measured ozone concentrations. With regard to SOA yields, it has been shown that model predictions based on simulation chamber yields dramatically underestimate SOA formation in the polluted atmosphere (*31*). Recently determined SOA yields (e.g., ref *55*) close the gap somewhat, but a significant discrepancy still remains. Scaling up the modeling SOA estimates (*47*−*51*) by the measurement/model discrepancies summarized in ref *31* would produce SOA fractions of the order of those in this study. Additionally, estimates based on EC-tracer method calculations could be biased low due to difficulties estimating $(OC/EC)_p$ with the ambient regression method. Previous studies using the EC-tracer method in the LA basin have obtained SOA/OA ≤ 50% using $(OC/EC)_p \geq 2$. As discussed earlier, this is likely an overestimate with more realistic values being ~1.4 or lower. Recalculating the results of Polidori et al. (*21*) using an $(OC/EC)_p = 1.4$ increases the SOA/OA to ~65%. Recalculating results from other studies which applied the EC-tracer method is not possible due to a lack of reported data.

Another possible reason for the observed differences is that the fraction of SOA in the LA basin may have increased with time via, e.g., more efficient POA emissions reduction (due to targeted policies such as vehicle emission controls), than reduction of SOA precursors (*28*). Although VOCs generally have been targeted by emission control policies with the main goal of reducing $O_3$ formation, the dominant precursors and pathways of SOA formation in urban areas are very unclear at present (*31*), so it is difficult to evaluate the impact of previous air quality improvement policies in SOA relative to POA.

Our estimates from SOAR-1 indicate that the composition of OA at the eastern part of the LA Basin is dominated by SOA by a wide margin, and that these results likely extend to the western part of the basin as well. Contributions from POA are significantly smaller and are similar to SOA only during the morning rush hour. These high contributions from SOA also occurred absent severe photochemical smog events. Source apportionment of OA is important to regulatory strategies involved with protecting air quality and human health. These efforts have put more emphasis on controlling direct POA emissions than emissions of SOA precursor gases. Our results strongly suggest that this strategy should be reconsidered due to the overwhelming contribution of SOA to OA during the summer in the LA basin.

## Acknowledgments

We acknowledge funding provided by U.S. Environmental Protection Agency (EPA) STAR grants RD832161010 and R831080, National Science Foundation (NSF) grant ATM-0449815, and NSF/UCAR grant S05-39607. P.F.D. and I.M.U. were supported by EPA Fellowship FP-9165081 and NASA Fellowship NNG05GQ50H, respectively. We also thank Megan McKay and Allen Goldstein for the use of their CO measurements in the CO-tracer calculations, and the rest of the Jimenez group and Aerodyne Research for support in the field and helpful discussions. We would also like to thank Paul Ziemann and the Air Pollution Research Center for hosting the SOAR-1 study. The United States Environmental Protection Agency through its Office of Research and development collaborated in the research described here. It has been subjected to Agency review and approved for publication. Mention of trade names or commercial products does not constitute endorsement or recommendation for use.

## Supporting Information Available

Figures S1−S7 and Tables S1 and S2. This material is available free of charge via the Internet at http://pubs.acs.org.

## Literature Cited

(1) Zhang, Q.; et al. Ubiquity and dominance of oxygenated species in organic aerosols in anthropogenically-influenced Northern Hemisphere midlatitudes *Geophys. Res. Lett.* **2007**, *34*, L13801, doi: 10.1029/2007GL029979.

(2) Schauer, J. J.; et al. Source apportionment of airborne particulate matter using organic compounds as tracers. *Atmos. Environ.* **1996**, *30*, 3837–3855.

(3) American Lung Association's State of the Air, 2007, http://lungaction.org/reports/sota07_cities.html.

(4) Synder, D. C.; Schauer, J. J. An inter-comparison of two black carbon aerosol instruments and a semi-continious elemental carbon instrument in the urban environment. *Aerosol Sci. Technol.* **2007**, *41*, 463–474.

(5) Grover, B. D.; et al. Semi-continuous mass closure of the major components of fine particulate matter in Riverside, CA. *Atmos. Environ.* **2008**, *42*, 250–260.

(6) Stone, E. A.; et al. Source apportionment of fine organic aerosol in Mexico City during the MILAGRO Experiment 2006. *Atmos. Chem. Phys.* **2008**, *8*, 1249–1259.

(7) Peltier, R. E.; et al. Investigating a liquid-based method for online organic carbon detection in atmospheric particles. *Aerosol Sci. Technol.* **2007**, *41*, 1117–1127.

(8) DeCarlo, P. F.; et al. Field-deployable, high-resolution, time-of-flight aerosol mass spectrometer. *Anal. Chem.* **2006**, *78*, 8281–8289.

(9) Turpin, B. J.; Lim, H. J. Species contributions to PM2.5 mass concentrations: Revisiting common assumptions for estimating organic mass. *Aerosol Sci. Technol.* **2001**, *35*, 602–610.

(10) Sueper, D., ToF-AMS High Resolution Analysis Software—Squirrel, http://cires.colorado.edu/jimenez-group/ToFAMSResources/ToFSoftware/SquirrelInfo/.

(11) Salcedo, D.; et al. Characterization of ambient aerosols in Mexico City during the MCMA-2003 campaign with Aerosol Mass Spectrometry: results from the CENICA Supersite. *Atmos. Chem. Phys.* **2006**, *6*, 925–946.

(12) Canagaratna, M.; et al. Chemical and microphysical characterization of ambient aerosols with the Aerodyne Aerosol Mass Spectrometer. *Mass Spectrom. Rev.* **2007**, *26*, 185–222.

(13) Slowik, J. G.; et al. Particle morphology and density characterization by combined mobility and aerodynamic diameter measurements. Part 2: Application to combustion-generated soot aerosols as a function of fuel equivalence ratio. *Aerosol Sci. Technol.* **2004**, *38*, 1206–1222.

(14) Jimenez, J. L.; et al. Ambient aerosol sampling using the Aerodyne Aerosol Mass Spectrometer *J. Geophys. Res.-Atmos* **2003**, *108* 8425, doi: 10.1029/2001JD001213.

(15) Paatero, P.; Tapper, U. Positive matrix factorization-A nonnegative factor model with optimal utilization of error-estimates of data values. *Environmetrics* **1994**, *5*, 111–126.

(16) Ulbrich, I.; et al. Interpretation and of organic components from Positive Matrix Factorization of Aerosol Mass Spectrometric data. *Atmos. Phys. Chem. Discussions* **2008**, *8*, 6729–6791.

(17) Lanz, V. A.; et al. Source apportionment of submicron organic aerosols at an urban site by factor analytical modelling of aerosol mass spectra. *Atmos. Chem. Phys.* **2007**, *7*, 1503–1522.

(18) Phuleria, H. C.; et al. Air quality impacts of the October 2003 Southern California wildfires *J. Geophys. Res.-Atmos.* **2005**, *110*, D07S20, doi: 10.1029/2004JD004626.

(19) Prather, K. A. personal communication. **2007**.

(20) Turpin, B. J.; Huntzicker, J. J. Identification of secondary organic aerosol episodes and quantitation of primary and secondary organic aerosol concentrations during SCAQS. *Atmos. Environ.* **1995**, *29*, 3527–3544.

(21) Polidori, A.; et al. Indoor/outdoor relationships, trends, and carbonaceous content of fine particulate matter in retirement homes of the Los Angeles basin. *J. Air Waste Manage Assoc.* **2007**, *57*, 366–379.

(22) Strader, R.; et al. Evaluation of secondary organic aerosol formation in winter. *Atmos. Environ.* **1999**, *33*, 4849–4863.

(23) Zhang, Q.; et al. Hydrocarbon-like and oxygenated organic aerosols in Pittsburgh: insights into sources and processes of organic aerosols. *Atmos. Chem. Phys.* **2005**, *5*, 3289–3311.

(24) Harley, R. A.; et al. Changes in motor vehicle emissions on diurnal to decadal time scales and effects on atmospheric composition. *Environ. Sci. Technol.* **2005**, *39*, 5356–5362.

(25) CARB Emissions data for South Coast Air Basin, 2005, http://www.arb.ca.gov/ei/emissiondata.html.

(26) Kirchstetter, T. W.; et al. On-road measurement of fine particle and nitrogen oxide emissions from light- and heavy-duty motor vehicles. *Atmos. Environ.* **1999**, *33*, 2955–2968.

(27) Allen, J. O.; et al. Emissions of size-segregated aerosols from on-road vehicles in the Caldecott Tunnel. *Environ. Sci. Technol.* **2001**, *35*, 4189–4197.

(28) Ban-Weiss, G. A.; et al. Long-term changes in emissions of nitrogen oxides and particulate matter from on-road gasoline and diesel vehicles. *Atmos. Environ.* **2008**, *42*, 220–232.

(29) Cabada, J. C.; et al. Estimating the secondary organic aerosol contribution to $PM_{2.5}$ using the EC tracer method. *Aerosol Sci. Technol.* **2004**, *38*, 140–155.

(30) Szidat, S.; et al. Contributions of fossil fuel, biomass-burning, and biogenic emissions to carbonaceous aerosols in Zurich as traced by C-14 *J. Geophys. Res., [Atmos]* **2006**, *111*, D07206, doi: 10.1029/2005JD006590.

(31) Volkamer, R.; et al. Secondary organic aerosol formation from anthropogenic air pollution: Rapid and higher than expected *Geophys. Res. Lett.* **2006**, *33*, 17, L17811, doi: 10.1029/2006GL026899.

(32) Takegawa, N.; et al. Seasonal and diurnal variations of submicron organic aerosol in Tokyo observed using the Aerodyne aerosol mass spectrometer *J. Geophys. Res., [Atmos]* **2006**, *111*, D11206, doi: 10.1029/2005JD006515.

(33) de Gouw, J. A.; et al. Budget of organic carbon in a polluted atmosphere: Results from the New England Air Quality Study in 2002 *J. Geophys. Res., [Atmos]* **2005**, *110*, D16305, doi: 10.1029/2004JD005623.

(34) Kleeman, M. J.; et al. Source contributions to the size and composition distribution of atmospheric particles: Southern California in September 1996. *Environ. Sci. Technol.* **1999**, *33*, 4331–4341.

(35) Griffin, R. J.; et al. Contribution of gas phase oxidation of volatile organic compounds to atmospheric carbon monoxide levels in two areas of the United States *J. Geophys. Res., [Atmos]* **2007**, *112*, D10S17, doi: 10.1029/2006JD007602.

(36) Weber, R. J.; et al. A study of secondary organic aerosol formation in the anthropogenic-influenced southeastern United States *J. Geophys. Res., [Atmos]* **2007**, *112*, D13302, doi: 10.1029/2007JD008408.

(37) Kondo, Y.; et al. Oxygenated and water-soluble organic aerosols in Tokyo *J. Geophys. Res., [Atmos]* **2007**, *112*, D01203, doi: 10.1029/2006JD007056.

(38) Favez,O.; et al. Significant formation of water-insoluble secondary organic aerosol in semi-arid urban environment *Geophys. Res. Lett.* **2008** *35*, L15801, doi: 10.1029/20086L034446.

(39) Sannigrahi, P.; et al. Characterization of water-soluble organic carbon in urban atmospheric aerosols using solid-state C-13 NMR spectroscopy. *Environ. Sci. Technol.* **2006**, *40*, 666–672.

(40) Rogge, W. F.; et al. Sources of fine organic aerosol 2. Noncatalyst and catalyst-equipped automobiles and heavy-duty diesel trucks. *Environ. Sci. Technol.* **1993**, *27*, 636–651.

(41) Simoneit, B. R. T.; et al. Levoglucosan, a tracer for cellulose in biomass burning and atmospheric particles. *Atmos. Environ.* **1999**, *33*, 173–182.

(42) Zheng, M.; et al. Source apportionment of $PM_{2.5}$ in the southeastern United States using solvent-extractable organic

compounds as tracers. *Environ. Sci. Technol.* **2002**, *36*, 2361–2371.
(43) Reff, A.; et al. Receptor modeling of ambient particulate matter data using positive matrix factorization: Review of existing methods. *J. Air Waste Manage Assoc.* **2007**, *57*, 146–154.
(44) Zhang, Q.; et al. Deconvolution and quantification of hydrocarbon-like and oxygenated organic aerosols based on aerosol mass spectrometry. *Environ. Sci. Technol.* **2005**, *39*, 4938–4952.
(45) Kroll, J. H. Evolution of Diesel Exhaust Aerosol in an Urban Environment, EOS Transactions AGU, Fall Meeting Supp., paper A31E-02, 2007.
(46) Aiken, A.; et al. O/C and OM/OC ratios of primary, secondary, and ambient organic aerosols with high resolution time-of-flight mass spectrometry. *Environ. Sci. Technol.* **2008**, *42*, 4478–4485.
(47) Pandis, S. N.; et al. Secondary organic aerosol formation and transport. *Atmos. Environ. A* **1992**, *26*, 2269–2282.
(48) Hildemann, L. M.; et al. Mathematical-modeling of urban organic aerosol—Properties measured by high-resolution gas-chromatography. *Environ. Sci. Technol.* **1993**, *27*, 2045–2055.
(49) Griffin, R. J.; et al. Secondary organic aerosol - 3. Urban/regional scale model of size- and composition-resolved aerosols *J. Geophys. Res., [Atmos]* **2002**, *107*, 4334, doi: 10.1029/2001JD000544.
(50) Vutukuru, S.; et al. Simulation and analysis of secondary organic aerosol dynamics in the South Coast Air Basin of California *J. Geophys. Res., [Atmos]* **2006**, *111*, 13, D10S12, doi: 10.1029/2005JD006139.
(51) Ying, Q.; et al. Verification of a source oriented externally mixed air quality model during a severe photochemical smog episode. *Atmos. Environ.* **2007**, *41*, 1521–1538.
(52) Schauer, J. J.; et al. Source reconciliation of atmospheric gas-phase and particle-phase pollutants during a severe photochemical smog episode. *Environ. Sci. Technol.* **2002**, *36*, 3806–3814.
(53) Appel, B. R.; et al. Analysis of carbonaceous material in Southern California atmospheric aerosols. 2. *Environ. Sci. Technol.* **1979**, *13*, 98–104.
(54) Herndon, S. C.; et al. The correlation of secondary organic aerosol with odd oxygen in a megacity outflow *Geophys. Res. Lett.* **2007**, *35*, L15804, doi: 10.1029/2008Gl034058.
(55) Ng, N. L.; et al. Secondary organic aerosol formation from *m*-xylene, toluene, and benzene. *Atmos. Chem. Phys.* **2007**, *7*, 3909–3922.

ES8008166